

REGIONAL MODELING AND POWER SPECTRA OF MERCURY'S CRUSTAL MAGNETIC FIELD.

A. M. Plattner¹ and C. L. Johnson^{2,3}, ¹Dept. of Earth and Environmental Sciences, California State University, Fresno, CA 93740, USA. aplattner@csufresno.edu, ²Dept. of Earth, Ocean and Atmospheric Sciences, University of British Columbia, Vancouver, BC, V6T 1Z4, Canada. ³Planetary Science Institute, Tucson, AZ 85719, USA.

Overview: Mercury's magnetic field recorded by the MErcury Surface, Space ENvironment, GEochemistry, and Ranging (MESSENGER) satellite mission contains a crustal component first described by [1]. Data at sufficiently low altitudes to successfully measure the weak crustal field are only available for latitudes north of $\sim 30^\circ\text{N}$ because of MESSENGER's highly eccentric orbit. As a consequence, regional methods are required to invert for crustal magnetic field models. Here we present models obtained using two different approaches: altitude-cognizant gradient vector Slepian functions (AC-GVSF) as described by [2] using the software available from [3], and equivalent-source dipoles (ESD) [4]. The two models shown in Fig. 1 differ in their fine-detail structure but reveal the same large- and medium-scale patterns. For each of the models, we calculated a regional Mauersberger-Lowes power spectrum using the method of [5] for latitudes 45°N to 72°N and for three spherical caps, each covering a distinct region (Fig. 2).

Crustal Magnetic Field Modeling: Mercury's magnetic field is dominated by contributions from the core dynamo and from magnetospheric current systems. We remove these by subtracting the magnetospheric model of [6] and then using an orbit-by-orbit along-track filter [1]. The data cover our modeling region unevenly as the track-to-track distance at lower latitudes is substantially greater than that near the poles. To avoid model artifacts from uneven sampling, we randomly subsampled the data 200 times using an equal-area approach. For each of the 200 data sets, we calculated, and then averaged, individual AC-GVSF models for latitudes 45°N to 72°N (Fig. 1, left). We used the same approach to obtain a mean ESD model for the region north of 38°N (Fig. 1, right).

Regional Power Spectra: For both the AC-GVSF model and the ESD model, we calculated regional power spectra using the approach described by [5]. Fig. 2 shows the spectra for the area between latitudes 45°N to 72°N ("ring") and for the spherical caps indicated in Fig. 1. The AC-GVSF model (solid) focuses on the spherical-harmonic degrees up to 110 and minimizes contributions from the more noise-sensitive higher degrees, whereas the ESD model (dashed) evenly distributes the model energy over the higher degrees. The "meridian" region is weakly magnetized. The "Rustaveli" region is similar but with more energy at the wavelengths associated with the Rustaveli Basin.

Decorrelation depths [7] are consistent with crustal sources in these regions. The "Caloris" region, north of the Caloris Basin, contains more energy in the low spherical-harmonic degrees, indicating that the magnetic sources are either at greater depths, or are spatially correlated over large areas, e.g., Caloris impact melt or ejecta. The "ring" spectrum is a superposition of the spectra for the distinct regions.

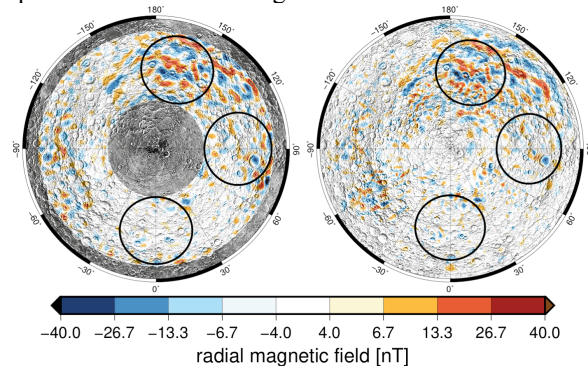


Figure 1. Left: Mean AC-GVSF model, right: mean ESD model. Both radial crustal magnetic field models are projected onto the planet's surface approximated by a sphere of radius 2440 km. Black circles denote the regions for the power spectra in Fig. 2: "Caloris" (165°E), "Rustaveli" (90°E), "meridian" (0°E).

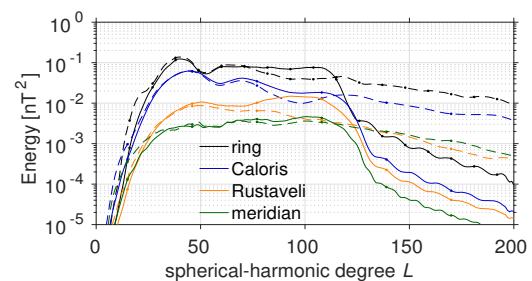


Figure 2. Regional power spectra for latitudes 45°N to 72°N ("ring") and the 13° spherical caps shown in Fig. 1. Solid lines are for the AC-GVFS model (Fig. 1, left), dashed lines for the ESD model (Fig. 1, right).

References: [1] Johnson C. L. et al. (2015) *Science*, 348, 892. [2] Plattner A. and Simons F. J. (2017) *GJI*, 211, 207-238. [3] Plattner A. (2017), doi: 10.5281/zenodo.583624. [4] Langel R. A. and Hinze W. J. (1998). [5] Wiczcerek M. A. and Simons F. J. (2005) *GJI*, 162, 655-675. [6] Korth H. et al. (2017) *GRL*, 44, 10147-10154. [7] Voorhies C. V. et al. (2002), *JGR*, 107, E6, 5034.